JOC The Journal of Organic Chemistry

Article

pubs.acs.org/joc

A C_{3v}-Symmetric Tripodal Urea Receptor for Anions and Ion Pairs: Formation of Dimeric Capsular Assemblies of the Receptor during Anion and Ion Pair Coordination

Arghya Basu and Gopal Das*

Department of Chemistry, Indian Institute of Technology, Guwahati, Assam 781039, India

Supporting Information

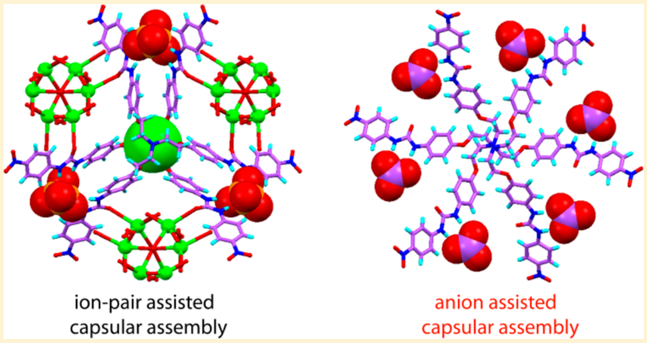

ABSTRACT: A new C_{3v}-symmetric urea-based heteroditopic tripodal receptor capable of recognizing both anions and ion pairs was designed, synthesized, and characterized. The protonated receptor forms a sulfate complex which encapsulates a single DMF in the tripodal cavity of the receptor. However, the SO_4^{2-} anion is located outside the tripodal cavity and is stabilized by N−H···O hydrogen bonds from the urea functions of four receptor cations. With $TBAHSO_4$ the receptor forms a contact ion pair complex, where both the TBA^+ and SO_4^{2-} groups are pseudoencapsulated in the tripodal cavity of the protonated receptor. Significantly, the receptor forms a charge-separated polymeric ion pair complex with K^+ and HPO_4^{2-} via formation of a dimeric capsular assembly of the receptor, in which three K^+ encapsulated dimeric capsular assemblies interdigitate to form a precise cavity that further encapsulates HPO_4^{2-}. The receptor also forms an anion complex with CO_3^{2-} via formation of dimeric capsular self-assembly of the receptor. Solution-state binding studies of the receptor with oxyanions have also been carried out by ^1H NMR titration experiments, which show the oxyanion binding trend $HCO_3^- > H_2PO_4^- > HSO_4^-$, whereas no binding with NO_3^- and ClO_4^- anions is observed.

INTRODUCTION

In recent times, one of the most exciting areas in the field of host−guest chemistry is the design and synthesis of receptors capable of recognizing anions and ion pairs efficiently and selectively.[1] Recognition of anions and ion pairs by synthetic receptors is important because of their pivotal roles in biological, environmental, and industrial applications.[1,2] Among the various anions, recognition of oxyanions, especially carbonate, sulfate, and phosphate, has drawn much research attention due to their fundamental roles in synthetic, health care, environmental, and energy related problems.[2] For example, the harmful effect of sulfate has been recognized as a prominent troublesome species in cleanup processes of nuclear waste and hard water; e.g., contamination of nuclear waste sites by this anion has been a matter of increased concern, hampering the treatment process.[2a−c] In addition, phosphate is one of the fundamental ingredients in the fertilizer industry, as plants require phosphorus for growth, although inorganic phosphate also causes eutrophication in water resources.[2f−h] The transport of HCO_3^- across the cell membrane plays a crucial role in many physiological functions.[2l−n] Moreover, the alkali-metal salts of these anions have also emerged as desirable targets for molecular recognition, because in nature these anions exist mostly as their Na/K salts.[3]

On the other hand, the self-assembly of capsules is one of the most attractive fields in supramolecular chemistry due to its great number of applications.[4] Acyclic receptors with a multiarmed hydrogen-bonding functionality have often been found to coordinate with targeted anionic species via the formation of capsular assemblies.[5] In this regard TREN-based tris(urea) or -(thiourea) ligands represent a class of receptors that has proven particularly useful for recognition and separation of oxyanions through encapsulation.[5b] The TREN scaffold has been widely used in anion coordination chemistry, either in its protonated form or as a part of more complicated receptors. On the other hand, anion encapsulation can also be constructed with the help of metal coordination. Metal complexes allow for the preorientation of the building blocks according to the metal coordination geometry to offer a complementary binding environment for anions.[6] Considering these facts, herein we have developed the elongated C_{3v}-symmetric N-bridgehead flexible tripodal urea receptor **L** by deliberately positioning the cation binding/protonation site far from the anion binding site (Scheme 1). The receptor forms sulfate complex **1** in its protonated form, which has been structurally characterized and shows encapsulation of a neutral DMF guest molecule in the tripodal cavity of the protonated

Received: January 16, 2014
Published: February 24, 2014

Scheme 1. Synthetic Route of C_{3v}-Symmetric Heteroditopic Tripodal Urea Receptor

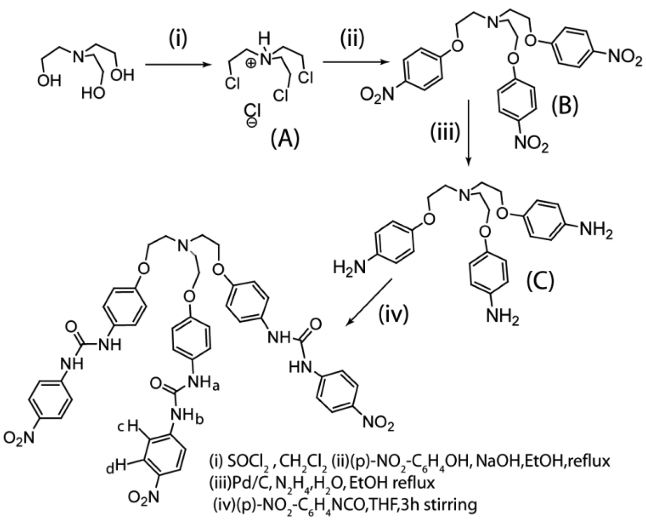

receptor and the SO_4^{2-} anion is situated outside of the tripodal cavity and stabilized by N−H···O hydrogen bonds from the urea functions of four receptor cations. In the case of $TBAHSO_4$ the receptor forms the unusual contact ion pair complex **2**, in which both the TBA cation and SO_4^{2-} anion are partially encapsulated in the distorted-C_{3v}-symmetric tripodal cavity of the protonated receptor. Further, the receptor forms the notable C_{3v}-symmetric charge-separated ion pair complex **3** with a potassium cation and hydrogen phosphate anion via formation of a dimeric capsular assembly of the receptor, where three nearby K^+ encapsulated dimeric capsular assemblies interdigitate to form a cavity to encapsulate the HPO_4^{2-} by six urea groups. Interestingly, in contrast to complex **3**, the receptor forms a distinct dimeric capsular self-assembly via C−H···π interactions while coordinating with a planar carbonate anion in the solid state. The solution-state binding of different oxyanions with the receptor **L** was also investigated in detail by ^1H NMR spectroscopy in d_6-DMSO at room temperature.

■ RESULTS AND DISCUSSION

The receptor was synthesized from previously reported tris(2-chloroethyl)amine hydrochloride (A) by simple S_N2 substitution with 4-nitrophenol in presence of NaOH in EtOH,[7] followed by reduction with Pd/C in EtOH to yield the corresponding triamine C (Scheme 1).[8] Subsequently, reaction of triamine C with 3 equiv of 4-nitophenyl isocyante in dry THF produced the desired receptor **L** in good yield. The ditopic receptor was thoroughly characterized by ^1H and ^{13}C NMR and IR spectroscopy, electrospray mass spectrometry, and single-crystal X-ray analysis.

For a receptor to bind with the ionic guests, it should, in principle, possess a proper binding site tailored to a suitable platform/framework. Receptor **L** possesses a highly organized tripodal scaffold with both cation and anion binding sites. In addition, functionalization of **L** with π-acidic nitrophenyl moieties as aryl terminals significantly enhances the binding ability of the receptor toward anionic guests.

Crystal Structure Description of the Receptor and Its Complexes. *Structural Description of Receptor **L**.* The ligand **L** crystallizes in triclinic space group $P\bar{1}$ with Z = 4 and Z′ = 2 together with four DMF and two water molecules (Figure 1).

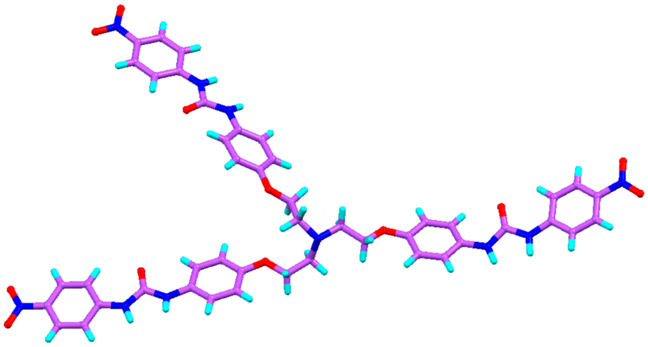

Figure 1. Molecular structure of receptor **L**. The other unit in the asymmetric unit and solvent molecules are omitted for clarity.

In supramolecular chemistry, the presence of more than one molecular conformer in the same crystal structure has been described by the term *conformational isomorphism*, and their occurrence is accounted for by thermodynamic and kinetic crystal stability, because these are mostly considered to be the result of an interrupted crystallization process. Crystal structure analysis of **L** shows that the three tripodal side arms of both conformational isomorphs (C1 and C2) are directed in three different directions with the absence of any intramolecular interactions, suggesting the unpreorganized nature of the tripodal receptor **L** in guest (anion/cation) free conditions. Probably the absence of intramolecular interactions makes the receptor flat and unpreorganized. For both conformers (C1 and C2) two urea functions form similar bifurcated hydrogen bonds with the oxygen atoms of two DMF molecules individually, whereas the third urea function forms bifurcated hydrogen bonds with the lattice water molecule which is further hydrogen bonded with the bridgehead nitrogen atom and the oxygen atom of a urea function of neighboring receptor molecules (Figure S23, Supporting Information). The donor−acceptor distances of these hydrogen bonds are <3.0 Å, and details of the hydrogen-bonding interactions involved in the crystal structure of **L** are provided in Table S1 in the Supporting Information. Furthermore, each receptor unit is linked to another adjacent unit of different symmetry via intermolecular C−H···O hydrogen-bonding interactions, donated from aromatic C−H protons to the oxygen atoms of the urea functions of an adjacent molecule. The crystal packing shows layered assembly formation (Figure S24, Supporting Information).

Structural Description of Complex 1. Complex **1** crystallizes in the triclinic space group $P\bar{1}$ with two protonated receptor moieties along with one sulfate anion, and four DMF and two water molecules as the solvents of crystallization. The structural elucidation reveals a 2:1 receptor:anion stoichiometric salt formation, confirming the SO_4^{2-} complex of protonated **L**. All three arms of the protonated receptor (**LH**$^+$) are projected in one direction. The O atoms of each aliphatic branch are nearly equidistant (~2.74 Å) from the bridgehead N atom, indicative of hydrogen-bonding interactions between the proton attached to the bridgehead N atom and O atoms of each aliphatic branch. These hydrogen-bonding interactions actually organize the flexible branches of the receptor in one direction. One ortho hydrogen atom of the aromatic ring attached to an ethereal oxygen atom of each branch is connected to a similar aromatic ring of a neighboring arm through a C−H···π interaction (Figure 2a) in a twisted edge-to-face fashion. The unidirectional arms of **LH**$^+$ create a tripodal cavity, which encapsulates a DMF solvent in its center,

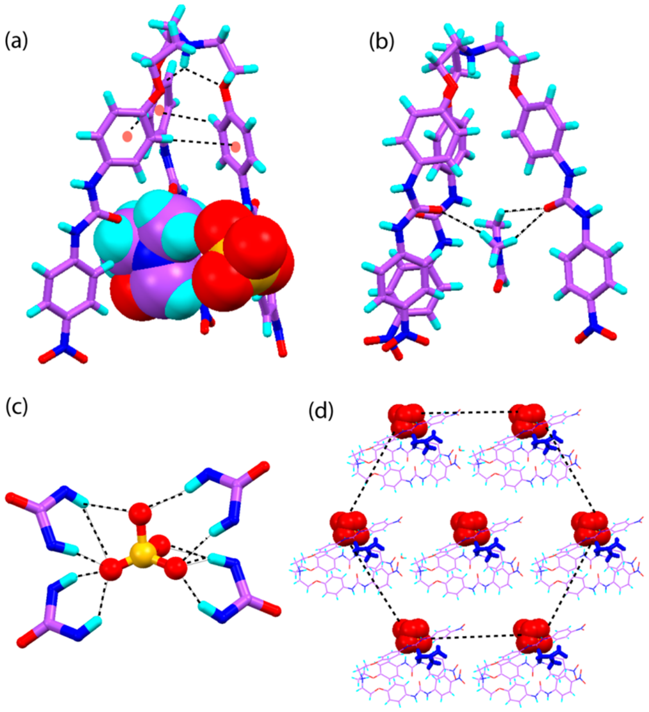

Figure 2. (a) X-ray structure of complex **1**, where the receptor molecule is shown as a stick model and the encapsulated DMF molecule and the sulfate anion are shown as space-filling models. The DMF and water molecules positioned outside the capsule are omitted for clarity. (b) Hydrogen-bonding interactions between the encapsulated DMF molecule with protonated receptor $\mathbf{LH}^+$ in complex **1**. (c) Magnified view showing coordination of SO_4^{2-} with the eight −NH groups in complex **1**. (d) Crystal packing in complex **1**, as viewed down the crystallographic *a* axis. The sulfate anion and DMF molecule are shown as space-filling and bold stick models (blue), respectively.

and the encapsulated DMF molecule is stabilized by the C−H···O hydrogen-bonding interactions with two inwardly directed C═O groups of the two urea functions of $\mathbf{LH}^+$ (Figure 2b). The distance measured between the bridgehead nitrogen atom of the protonated receptor ($\mathbf{LH}^+$) and the nitrogen atom of the encapsulated DMF solvent is 10.53 Å. The oxygen atom of the encapsulated DMF molecule is hydrogen-bonded with the crystallizing water molecule, which is further hydrogen-bonded with a urea function of $\mathbf{LH}^+$ and the next DMF molecule. The SO_4^{2-} anion in complex **1** is located outside the tripodal cavity and is stabilized mainly by N−H···O hydrogen bonds from the urea functions of four receptor cations. The coordination environment of the SO_4^{2-} group in complex **1** is shown in Figure 2c. The detailed coordination environment of SO_4^{2-} suggests that it is involved in side-cleft binding with four receptor cations via 12 hydrogen-bonding interactions comprised of 10 N−H···O and 2 C−H···O bonds having an average donor-to-acceptor distance of 3.058 Å (Table S1, Supporting Information). A correlation of N−H···O angle vs N−H···O distance shows that 8 out of 10 N−H hydrogen bonds are in the strong hydrogen-bonding interaction region of $d(\text{H}\cdots\text{O}) < 2.5$ Å, $d(\text{N}\cdots\text{O}) < 3.2$ Å, and N−H···O > 140°. Apart from these hydrogen bonds with the receptor cations, the sulfate anion also forms weak C−H···O hydrogen bonds with the encapsulated DMF molecule.

Structural Description of Complex 2. After several attempts, we were able to isolate single crystals of **L** with $TBAHSO_4$. Complex **2** crystallized in a triclinic crystal system with the $P\overline{1}$ space group. Single crystals of complex **2** were grown from acetone solvent with moderate yield upon very slow evaporation of a solution of **L** in the presence of excess $TBAHSO_4$. The asymmetric unit of complex **2** has a distorted-C_{3v}-symmetric cavity, which is evident from the difference in basal N···N distances of nitro groups (N4···N7 = 17.17 Å, N7···

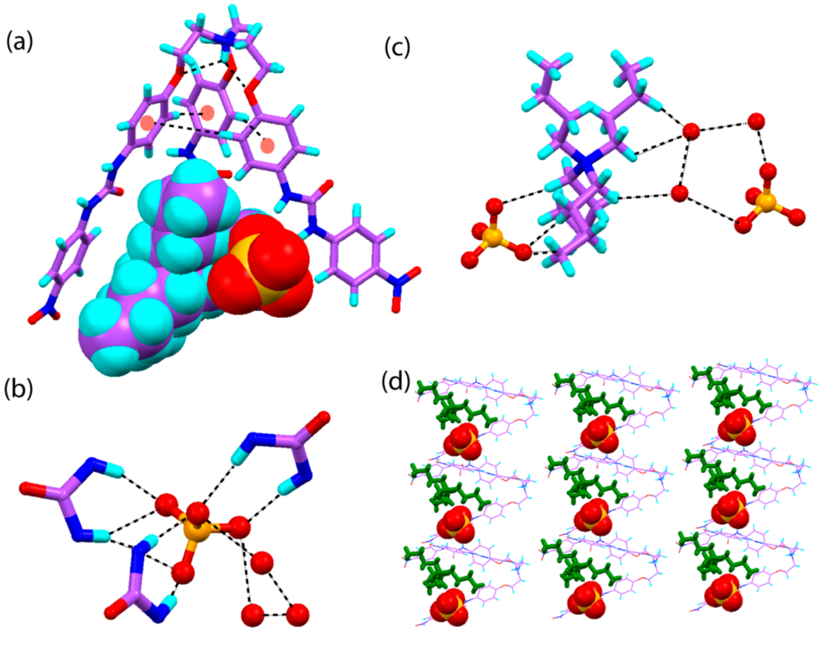

Figure 3. (a) X-ray structure of complex **2**, where the receptor molecule is shown as a stick model and the TBA cation and the sulfate anion are shown as space-filling models. (b) Hydrogen-bonding interactions of the sulfate anion with the urea functions of three receptor cations and crystallizing water molecules. (c) View showing the presence of both contact ion pair and solvent-separated ion pair interactions between the TBA cation and the sulfate anion in complex **2**. (d) Crystal packing in complex **2** as viewed down the crystallographic *c* axis. The sulfate anion is shown as a space-filling model, and the encapsulated TBA cation is shown as a bold stick model (dark green).

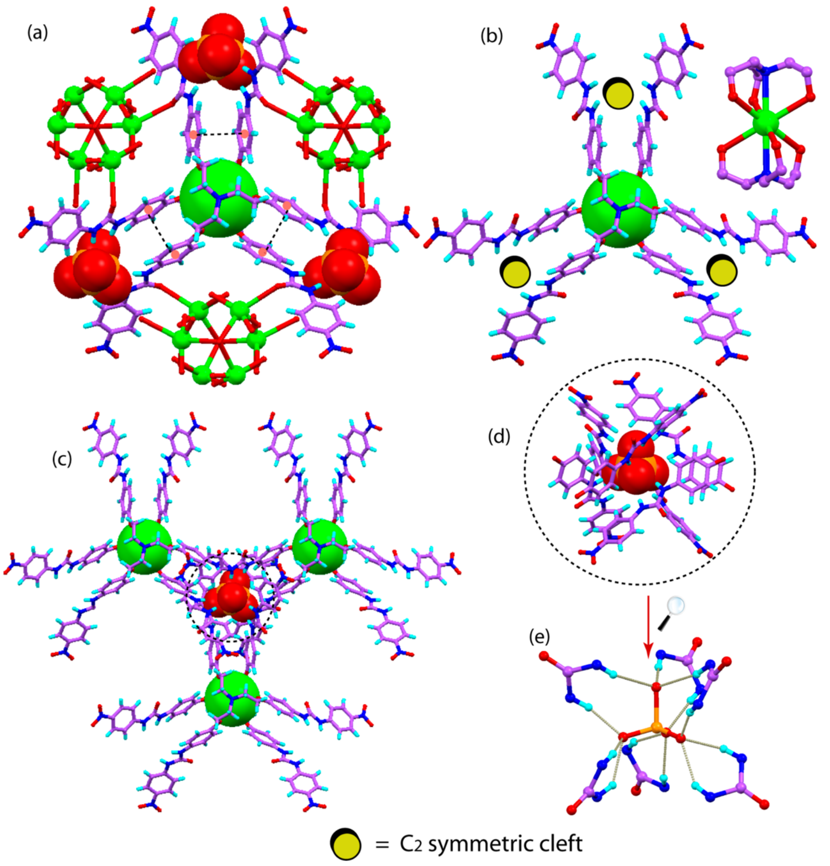

Figure 4. (a) C_{3v}-symmetric X-ray structure of complex **3**, where two receptor molecules are shown as stick models, the monohydrogen phosphate anion and the encapsulated potassium cation are shown as space-filling models, and the potassium cation binding to an oxygen atom of a urea function is shown as a ball and stick model. (b) View showing the encapsulation of K_1^+ within the dimeric capsular assembly of two symmetry-identical molecules of L and generation of three C_2-symmetric clefts. The inset shows the coordination mode of the encapsulated potassium cation with the two receptor molecules. (c) View showing three nearby K_1^+ encapsulated dimeric capsular assemblies interdigitating to form a precise cavity to encapsulate the HPO_4^{2-} anion. (d) Encapsulation of hydrogen phosphate anion by six urea functions. (e) Magnified view showing 12 hydrogen-bonding interactions between six urea functions and the hydrogen phosphate anion.

N10 = 10.63 Å, and N10···N4 = 9.58 Å). Close inspection of the crystal structure of complex **2** reveals that the receptor is protonated. Along with three crystallizing water molecules, the asymmetric unit of complex **2** contains one protonated receptor **LH**$^+$, one SO_4^{2-} anion, and one TBA countercation to balance the overall charge. The solution-state deprotonation of HSO_4^- can be explained due to the formation of multiple hydrogen-bonding interactions with the neutral receptor **L** that lowers the pK_a of the bound HSO_4^- to the extent that it is deprotonated by a bridgehead nitrogen atom of the receptor molecule **L** and becomes protonated (Figure 3). To the best of our knowledge, crystallographic evidence for proton transfer phenomena from a hydrogenated anion to a receptor in an ion pair complex has not been reported. However, solution-state deprotonation of the protonated state of an anion, viz. $H_2PO_4^-$, HCO_3^-, and HSO_4^-, and subsequent formation of a complex with deprotonated anions in the solid state is not uncommon.[6d−f] Similar to the case for complex **1** here also all three arms of **LH**$^+$ are projected in one direction and each ethereal O atom of an **LH**$^+$ unit is hydrogen-bonded to the proton attached to the bridgehead N atom that actually arranges the flexible arms in one direction (Figure 3a). The unidirectional tripodal arms of **LH**$^+$ create a distorted-C_{3v}-symmetric tripodal cavity, which encapsulates the TBA cation fully and the SO_4^{2-} anion partially as a contact ion pair in its center (Figure 3a,c). The encapsulated TBA cation is stabilized by cation···π, C−H···π, and C−H···O interactions with the phenyl rings and the urea functions of two side arms of the protonated tripodal receptor **LH**$^+$. The distance measured between the bridgehead nitrogen atoms of **LH**$^+$ and the TBA countercation is 11.616 Å. A closer look at the coordination environment of SO_4^{2-} suggests that it is stabilized by 14 hydrogen bonds involving 7 N−H···O (2 urea functions.) 2 O−H···O (lattice water molecules). 2 C−H···O (aryl −CH of nitrophenyl ring). and 3 C−H···O (TBA cation) (Figure 3b). Moreover, a detailed analysis of the hydrogen bond parameters, especially the N−H···O angle vs H···O distances, reveals that in the strong hydrogen bonding interaction region of d(N···O) ≤ 3.2 Å there are 8 contacts. The detailed hydrogen-bonding parameters are given in Table S1 in the Supporting Information.

Structural Description of Complex ***3***. The reaction of K_2HPO_4 with **L** in a 2/1 DMSO/H_2O binary mixture afforded complex **3**, as determined by X-ray diffraction. Complex **3** crystallizes in the trigonal system with centrosymmetric space group $P\overline{3}_1c$. The symmetric molecular structure of complex **3** is shown in Figure 4a. The crystal structure of **3** shows that the two potassium cations (K_1^+ and K_2^+) are present in different environments. The K_1^+ is encapsulated by two receptor molecules, where two of the same symmetric receptor molecules are flipped inward toward each other in a face-to-face fashion (d(N1⋯N1′) = 5.794 Å) and each receptor coordinates K_1^+ via three ethereal oxygen atoms and a bridgehead nitrogen atom with O⋯K_1^+ and N⋯K_1^+ distances of 2.962 and 2.899 Å, respectively (Figure 4b). The two receptors in this capsular assembly are assembled by weak $\pi\cdots\pi$ interactions of phenyl rings (C1g⋯C1′g = 3.579 Å) attached to the ethereal oxygen atoms (Figure 4a). However, K_2^+ is coordinated with oxygen atoms of a urea function and five water molecules (disordered). Two out of five water molecules are further coordinated to the next similar potassium cations to eventually form a C_3-symmetric $[K_6(H_2O)_5]^{6+}$ cluster (Figure 4a). Notably, the receptor does not recognize the K_2^+ in a convincing fashion; therefore, the presence of K_2^+ in the crystal lattice of complex **3** is only due to the balance of overall charge of the complex. The K_1^+ encapsulated dimeric capsular assembly of the receptor forms three C_2-symmetric clefts (Figure 4b). Three such clefts of three nearby K_1^+ encapsulated dimeric capsular complexes are aligned in such a way to create an anion-specific microcavity that further encapsulates a HPO_4^{2-} anion in its center via hydrogen-bonding participation of six urea functions (Figure 4c,d), which eventually leads to the formation of a 2D polymeric structure (Figure S31, Supporting Information). Notably, the hydrogen phosphate anion is disordered over two positions with the eight half-occupied O atoms; due to disorder, it was not possible to locate the hydrogen atom on the phosphate anion. Interestingly, all six urea arms within a capsule participate in hydrogen bonding with the encapsulated hydrogen phosphate ion. There are total of 12 hydrogen-bonding interactions (Figure 4e) between 6 urea functions of **L** moieties and 4 O atoms of one HPO_4^{2-} ion. Each oxygen atom of the hydrogen phosphate anion behaves as a trifurcated hydrogen bond acceptor, and each −NH group donates one N−H⋯O bond, resulting in 12 hydrogen bonds with an average donor-to-acceptor distance of 2.811 Å (Table S1, Supporting Information). Moreover, several weaker interactions involving aryl −CH protons could be added to the encapsulated HPO_4^{2-} anion when the donor-to-acceptor distance is limited to <3.5 Å for hydrogen bonding, which provides additional stability for hydrogen phosphate binding. As the urea functions of the K_1^+ encapsulated dimeric capsular assembly of the receptor form strong hydrogen-bonding interactions with hydrogen phosphate anion, therefore, the formation of a capsular assembly of the tripodal receptor **L** is not solely due to potassium cation coordination; rather, it is a combined coordination effect of potassium cation (encapsulated) and hydrogen phosphate anion. Hence, the receptor **L** forms an ion pair induced capsular assembly. It is important to mention here that efforts have also been made to crystallize sulfate and phosphate complexes of other alkali metals (Li^+ and Na^+), but in spite of several attempts, we were unable to form crystals. This is due to the smaller size and lower coordination number of Li^+/Na^+ (in comparison to K^+), which might not able to create stable preorganize encapsulation space for anion (sulfate and phosphate) upon coordination with the receptor **L**.

The ideal binding mode for tetrahedral oxyanions (sulfate and phosphate) is encapsulation of the anion via 12 optimally arranged binding sites.[2a−c,f,9] A detailed crystallographic analysis of complexes **1**−**3** shows that the metal-free receptor (in case of complexes **1** and **2**) is not able to provide an ideal binding site for these tetrahedral oxyanions (Figures 2b and 3c). However, in case of complex **3** the K_1^+ coordinated preorganized receptor provides an almost ideal binding site for the tetrahedral oxyanion through an assembly process (Figure 4e).

*Structural Description of Complex **4**.* Red block-shaped crystals of the carbonate complex suitable for single-crystal X-ray diffraction analysis were obtained after 5 days of slow evaporation of a DMSO solution of the receptor **L** in the presence of excess $TEAHCO_3$. The complex crystallized in the trigonal space group $R\overline{3}$ with Z = 6. The symmetric molecular structure of complex **4** is shown in Figure 5. In the crystal structure of complex **4**, two tripodal units self-assemble to form a molecular capsule (**L**$_2$) via intermolecular C−H⋯π interactions. Each of the two molecules of **L** in the crystal structure of the complex **4** is stabilized in a staggered conformation. Two units of **L** in complex **4** are flipped inward toward each other in a face-to-face fashion (d(N1⋯N1) = 3.970 Å) and held together via C−H⋯π interactions (d(C−H⋯π) 3.34 Å) from the ortho C−H of the aromatic ring, creating a cavity inside the capsule (Figure 5a and Figure S27, Supporting Information). Each arm of the molecular capsule is linked with that of a neighboring capsule through $\pi\cdots\pi$ stacking ($d(\pi\cdots\pi)$ = 3.72 Å). A similar type of dimeric capsular self-assembly formation in the absence of any added guest by a bromo-substituted N-bridged tripodal receptor was previously shown by Sun.[4i] In contrast to the case for complex **3**, here in complex **4** the dimeric capsular assembly of the receptor does not form any C_2-symmetric clefts and also no ionic guest encapsulation (K_1^+ encapsulation in complex **3**) is observed within the dimeric capsular assembly of **L**. Each of the six urea functions of the dimeric capsular assembly of **L** in complex **4** forms hydrogen bonds with different carbonate anions, and each carbonate anion is stabilized via hydrogen-bonding interactions of three urea functions belonging to three different dimeric capsular assemblies of **L**, which eventually leads to the formation of an interesting 2D polymeric assembly where a planar hexagonal arrangement of the dimeric capsular assembly of the receptor is observed (Figure 6). This type of metal-free anion-directed self-assembled coordination polymer formation in a neutral receptor system has rarely been highlighted in the literature.[10] A close inspection of the hydrogen-bonding interactions between the carbonate anion and receptor molecules reveals that the carbonate is stabilized by nine hydrogen bonds in complex **4**: six of these hydrogen bonds are donated by the urea −NH groups and the other three by the aryl −CH protons of the nitrophenyl rings. Each oxygen atom of the carbonate anion behaves as a trifurcated hydrogen bond acceptor, resulting in nine hydrogen bonds with an average

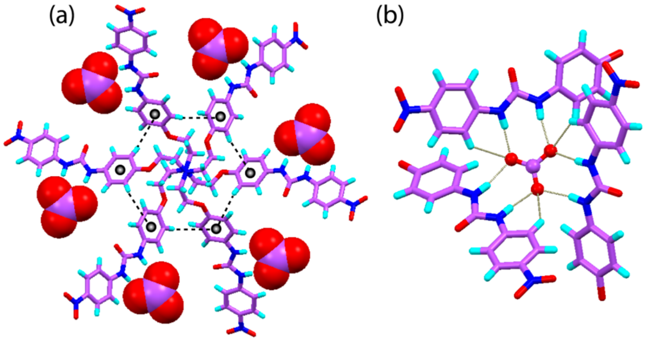

Figure 5. (a) C_{3v}-symmetric X-ray structure of complex **4**, where two receptor molecules are shown as stick models and carbonate anions are shown as space -filling models. (b) Magnified view showing that the carbonate anion is stabilized via nine hydrogen bonds with the receptor molecules in complex **4**.

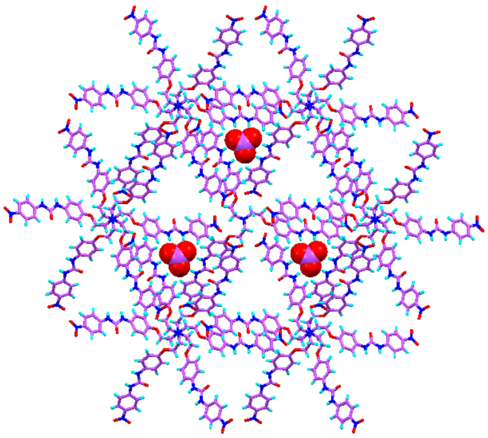

Figure 6. Carbonate anion coordination induced hexagonal arrangement of dimeric capsular assemblies of the receptor **L** in complex **4**.

donor-to-acceptor distance of 2.96 Å. The detailed hydrogen-bonding parameters are given in Table S1 in the Supporting Information.

^{1}H NMR Binding Studies. The binding properties of **L** with different oxyanions in solution have been both qualitatively and quantitatively investigated by performing ^{1}H NMR titration experiments in DMSO-d_6 at room temperature (Table 1). During titration experiments TBA salts of HSO_4^-, $H_2PO_4^-$, and CH_3COO^- have been used, while for HCO_3^- and NO_3^- anions TEA salts are used. The most significant changes in chemical shifts are observed for the urea protons of **L** with oxyanions, indicating the active participation of urea −NH protons in the solution-state binding events. The binding constants (log K_a) of the anions with **L** were determined with the EQNMR program.[11]

Table 1. Binding Constants (log *K*) for L with Different Oxyanions in DMSO-d_6 at Room Temperature[a]

anion	log K^b	host:guest	ΔG (kcal mol^{-1})
HSO_4^-	2.07 (K_{11})	1:1/2:1	−2.82
	3.51 (K_{21})		−4.78
$H_2PO_4^-$	2.77 (K_{11})	1:2	−3.77
	4.32 (K_{12})		−5.89
HCO_3^-	2.88 (K_{11})	1:2	−3.92
	4.83 (K_{12})		−6.58

[a]The NH resonances were followed for calculating log *K*. [b]Errors <15%.

^{1}H NMR titration of the receptor **L** with $TBAHSO_4^-$ shows that upon gradual addition of standard HSO_4^- solution a moderate downfield shift of urea −NH resonances ($\Delta\delta(-NH_a)$ = 0.574 ppm; $\Delta\delta(-NH_b)$ = 0.634 ppm) and a small but important change in the chemical shift of the aryl $-CH_c$ protons, $\Delta\delta$ = 0.127, could be explained by the fact that the hydrogen sulfate anion also considerably interacts with the C−H_c proton in the solution state. During the titration experiments, the chemical shifts of all the protons in **L** kept changing until 1.0 equiv of HSO_4^- ions was added. The Job plot showed a maximum at 0.57 mol fraction value of **L**, suggesting the formation of both 1:1 and 2:1 host:guest complexes in solution (Figure 7a). Following the shift of the $-NH_a$ signal, the titration curve is best fitted for a 2:1 rather than a 1:1 receptor:anion complex, yielding an overall association constant (log K_{21}) for HSO_4^- of 3.51 (Figures S14 and S20, Supporting Information).

In contrast to the complicated 1:1 and 2:1 host:guest binding with HSO_4^- anion, the titration experiment of **L** with $H_2PO_4^-$ anion shows 1:2 host:guest binding stoichiometry, confirmed from a Job plot analysis (Figures 7b). Interestingly, the degree of downfield shift of both −NH resonances is higher in comparison to the hydrogen sulfate anion. The overall association constant (log K_{12}) of **L** with $H_2PO_4^-$ is calculated by following the shift of the $-NH_a$ signal during the titration experiment and is found to be 4.32 (Figures S15 and S21, Supporting Information).

The binding behavior of **L** with HCO_3^- (as its TEA salt) ion in solution was also studied. The evolution of the spectrum was not at all easy to follow in the ^{1}H NMR titration experiments, due to significant peak broadening of both urea NH protons. This is due to the binding-induced broadening of the −NH signals rather than deprotonation, which was supported by the formation of a hydrogen-bonded complex in solid state even in the presence of excess $TEAHCO_3^-$. The titration experiment revealed 1:2 (host:guest) binding modes (Figure 7c). However, the crystal structure of complex **4** (carbonate complex) showed polymeric association with the carbonate anion. This discrepancy between the binding stoichiometry in the solid state and solution is not uncommon and has been previously observed for many anion binding receptors. The overall association constant (log K_{12}) of **L** with HCO_3^- is found to be 4.83 (Figures S16 and S23, Supporting Information).

Finally, in the ^{1}H NMR titration of **L** with a standard CH_3COO^- solution, the −NH resonance experienced a significant downfield shift for the $-NH_a$ and $-NH_b$ signals, indicating effective participation of the urea −NH protons toward binding of this anion. Notably, the titration revealed 1:3 (host:guest) binding modes (Figure 7d). A similar type of 1:3 host:guest binding for the acetate anion by a tripodal receptor was previously reported by Ghosh and a co-worker.[5g] The 1:3 (host:guest) binding modes with planar acetate is due to the flexible nature of the receptor in solution, which perhaps allow multiple anions to interact with a single receptor via side cleft binding. However, in the presence of other oxyanions such as nitrate and perchlorate, no appreciable changes in the chemical shift values of the −NH resonances were observed, suggesting the noninteracting nature or very weak interactions with **L** (Figures S18 and S19, Supporting Information).

It is important to note that efforts were also made to evaluate the ion pair binding properties of the receptor **L** with the potassium salt of various oxyanions, but the negligible shift with subsequent peak broadening and precipitation problems during ^{1}H NMR titration experiments prevented us from doing so.

■ CONCLUSION

A new C_{3v}-symmetric flexible N-bridgehead heteroditopic tripodal urea receptor **L** containing both cation and anion binding sites has been prepared and characterized. The oxyanions and ion pair binding properties of the receptor **L** were studied in both the solid and solution states. The structural analysis of sulfate complex **1** of the protonated receptor shows encapsulation of a neutral solvent guest (DMF) within the tripodal cavity of the receptor. However, the SO_4^{2-} anion remains outside of the tripodal cavity and forms several N−H···O hydrogen bonds with the urea functions of four receptor cations. However, with $TBAHSO_4$ the receptor forms an uncommon contact ion pair complex (**2**). In complex **2**,

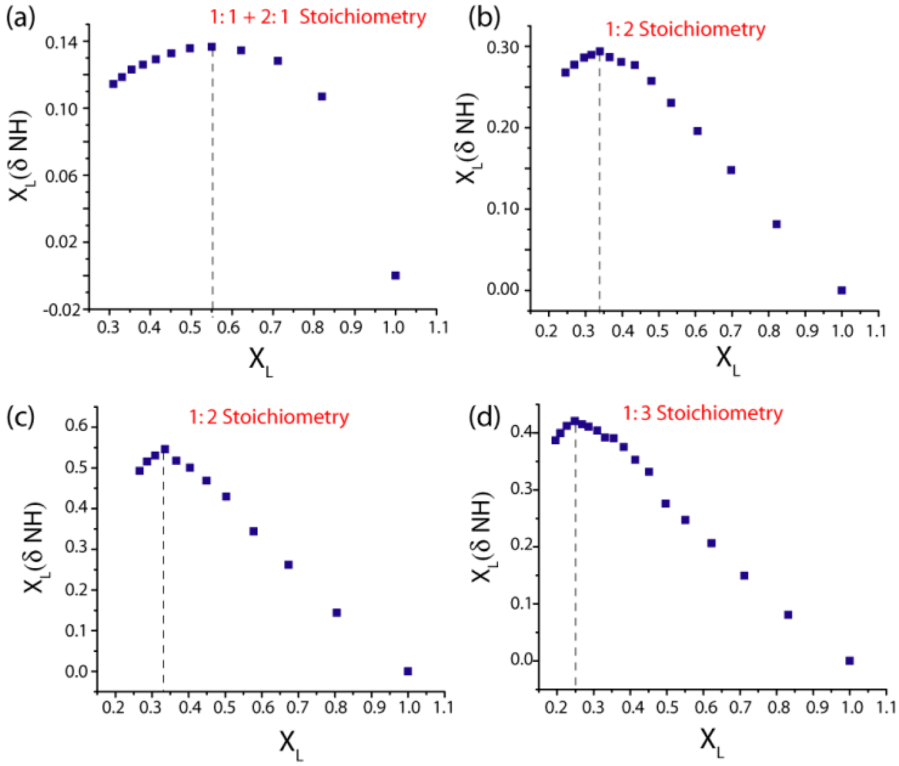

Figure 7. Job plots for **L** in DMSO-d_6 with different oxyanions: (a) hydrogen sulfate; (b) dihydrogen phosphate; (c) bicarbonate; (d) acetate.

both the TBA cation and SO_4^{2-} anion are pseudoencapsulated in the distorted-C_{3v}-symmetric tripodal cavity of the protonated receptor. Notably for ion pair complex **3**, the receptor forms a highly symmetric charge-separated 2D polymeric ion pair complex with a potassium cation and a hydrogen phosphate anion via formation of a dimeric capsular assembly of the receptor. In complex **3**, three C_2-symmetric clefts of three nearby K^+ encapsulated dimeric capsular assemblies interdigitize to form a microcavity that further encapsulates the hydrogen phosphate anion via hydrogen-bonding interactions with six urea groups. Moreover, the receptor also forms complex **4**, with a planar carbonate anion in its neutral form. Notably, on coordination with carbonate anion the receptor forms a dimeric capsular assembly, in which no ionic guest encapsulation is observed. This dimeric capsular assembly of the receptor in complex **4** further generates an interesting 2D polymeric assembly upon carbonate anion coordination. The structural comparison of complexes **3** and **4** suggests that, depending on the nature of the ionic guest, the receptor **L** forms two different types of dimeric capsular assemblies in the solid state. Solution state binding studies of **L** with different oxyanions have also been carried out by ^1H NMR in d_6-DMSO at room temperature. A detailed ^1H NMR study shows a 1:2 host:guest binding stoichiometry of HCO_3^- and $H_2PO_4^-$ anions with **L**, while 1:3 and both 1:1 and 2:1 host:guest binding stoichiometries are observed for CH_3COO^- and HSO_4^-, respectively. The binding constant calculations from ^1H NMR titration experiments of **L** with different oxyanions show the anion binding sequence $HCO_3^- > H_2PO_4^- > HSO_4^-$, whereas no binding with NO_3^- and ClO_4^- is observed.

■ EXPERIMENTAL SECTION

Materials and Methods. All reagents and solvents were obtained from commercial sources and used as received.

Instruments. IR spectra were recorded with KBr disks in the range 4000−400 cm^{-1}. All ^1H NMR spectra were recorded on a 400 MHz instrument. The ^{13}C NMR spectrum of the free receptor was recorded on a 300 MHz spectrometer. Chemical shifts were recorded in parts per million (ppm) with the solvent peak as reference. ESI-MS spectra were recorded with an LC-MS/MS system.

Synthesis and Spectral Characterization of the Receptor and Its Complexes. To a solution of 4-nitrophenol (15.3 g, 0.11 mol) in EtOH (80 mL) was added NaOH (5.98 g, 0.15 mol), and the solution was stirred at room temperature for 1 h (Scheme 1).[7] To the resulting solution was added tris(2-chloroethyl)amine hydrochloride (A; 8.0 g, 33.2 mmol) at once, and the mixture was refluxed for 10 h followed by removal of the solvents under reduced pressure and addition of 20 mL of cold water. The expected product was extracted from this mixture, with 3 × 30 mL of dichloromethane. The organic layer was washed three times with 10% K_2CO_3 solution and then two times with cold water and dried over anhydrous Na_2SO_4,, and the solvents were removed under reduced pressure. The crude product was purified by column chromatography (R_f = 0.48 in 30% ethyl acetate in petroleum ether). The desired compound B was a pale yellow solid. Yield: 65%.

Compound B (1.0 g, 1.95 mmol) was suspended in ethanol (100 mL) in a 250 mL round-bottomed flask. Then 5% Pd/C (50 mg, 5 wt %) was added to the suspension. Hydrazine hydrate (1.0 mL, 16 equiv) was added dropwise to this mixture. The mixture was refluxed for 10 h, followed by removal of the solvents under reduced pressure to give a colorless solid of the triamine C.[8] Yield: 85%.

A total of 492 mg (3.0 mmol) of 4-nitrophenyl isocyanate was dissolved in 30 mL of dry tetrahydrofuran (THF) in a 100 mL round-bottomed flask and 0.422 mg (1 mmol) of triamine C dissolved in 10 mL of dry THF was added dropwise (using a dropping funnel) over a period of 1 h with constant stirring at room temperature. The resulting solution mixture was stirred overnight at room temperature. Then, the volume of the solvent (THF) was reduced in vacuo by using a rotary evaporator, and the obtained solid product was filtered off and washed with 10 mL of dichloromethane a couple of times to remove the unreacted starting materials and impurities. The colorless precipitate was collected, dried in a desiccator, and characterized by NMR, FT-IR,

Table 2. Crystallographic Parameters and Refinement Details of Receptor L and Its Complexes (1−4)

param	**L**	**1**	**2**	**3**	**4**
formula	$C_{51}H_{58}N_{12}O_{15}$	C_{102} $H_{118}N_{24}O_{34}S$	$C_{61}H_{79}$ $N_{11}O_{19}S$	$C_{90}H_{84}K_2N_{20}O_{51}P$	$C_{46}H_{42}N_{10}O_{15}$
fw	1079.09	2256.27	1302.42	2369.36	974.90
cryst syst	triclinic	triclinic	triclinic	trigonal	trigonal
space group	$P\bar{1}$	$P\bar{1}$	$P\bar{1}$	$P\bar{3}_1c$	$R\bar{3}$
a (Å)	12.8085(4)	11.4144(6)	11.3397(10)	17.3549(9)	18.3034(14)
b (Å)	15.4038(5)	16.9099(11)	18.6819(17)	17.3549(9)	18.3034(14)
c (Å)	28.8727(12)	17.2091(11)	18.7690(16)	22.6324(12)	40.426(8)
α (deg)	84.217(3)	115.692(7)	103.700(3)	90.00	90.00
β (deg)	82.467(3)	100.539(5)	106.612(3)	90.00	90.00
γ (deg)	87.202(3)	98.828(5)	98.493(3)	120.00	120.00
V (Å^3)	5615.0(3)	2839.4(3)	3601.4(6)	5903.4(5)	11729(3)
Z	4	1	2	2	6
D_c (g cm^{-3})	1.276	1.319	1.201	1.334	0.828
μ (mm^{-1})	0.096	0.118	0.118	0.192	0.063
T (K)	298(2)	298(2)	298(2)	298(2)	298(2)
total no. of rflns	52642	23096	27840	16209	8797
no. of indep rflns	28571	14395	17883	5125	6625
no. of obsd rflns	18021	6871	8201	2213	5730
no. og params	1465	760	827	244	214
R1, wR2 ($I > 2\sigma(I)$)	0.0762, 0.2479	0.0838, 0.3383	0.0880, 0.2755	0.0966, 0.2740	0.0981, 0.2600
R(int)	0.0386	0.0278	0.2158	0.0992	0.0357
GOF (F^2)	0.934	1.052	1.067	1.034	0.995
CCDC no.	934175	934176	934177	934178	976675

ESI-MS. Yield: 82%. Mp: 194 °C ^{1}H NMR (d_6-DMSO): δ (ppm) 9.33 (s, 3H−N), 8.70 (s, 3H−N) 8.14 (d, 6H, J = 8.4 Hz, ArCH) 7.65 (d, 6H, J = 8.4 Hz, ArCH), 7.35 (d, 6H, J = 8 Hz ArCH), 6.88 (d, 6H, J = 8.4 Hz ArCH), 4.02 (s(br), 6H, NCH_2) 3.03 (s(br), 6H, NCH_2), ^{13}C NMR (d_6-DMSO): δ (ppm) 58.90, 71.92, 120.01, 122.48, 125.75, 130.36, 137.17 146.05, 151.79, 157.34, 159.41. FT-IR (ν, cm^{-1}): 1230 (C−N), 1333 (NO_2 sym), 1555 (NO_2 asym), 1607 (C=C), 1656 (−C=O), 3356 (N−H). ESI(+) mass spectrometry: calculated 915.31, found 915.33.

Complex **1** *(2**LH**$^+$·SO_4^{2-}·4DMF·2H_2O).* Complex **1** was obtained by adding 3 mL of an aqueous solution of Na_2SO_4 (14 mg, 1.0 mmol) to 8 mL of a DMF solution of the previously prepared perchlorate salt of receptor **L** (100 mg, 0.1 mmol). After the addition of aqueous Na_2SO_4, the mixture was stirred for about 1 h at room temperature. The resulting mixture was filtered into a 20 mL conical flask and allowed to slowly evaporate at room temperature, which yielded block-shaped pale yellow crystals suitable for X-ray crystallography analysis within 8−10 days. Mp: 146 °C, ^{1}H NMR (d_6-DMSO): δ (ppm) 9.577 (s, 3H−N), 8.969(s, 3H−N) 8.10 (d, 6H, J = 9.2 Hz, ArCH), 7.935 (s, 2H, DMF solvent) 7.67 (d, 6H, J = 9.2 Hz, ArCH), 7.39 (d, 6H, J = 8.8 Hz, ArCH), 6.88 (d, 2H, J = 9.2 Hz, ArCH), 4.25 (s(br), 6H, NCH_2) 3.51 (s(br), 6H, NCH_2), 2.874 (s, 6H, DMF solvent), 2.718 (s, 6H, DMF solvent). FT-IR (ν, cm^{-1}): 1214 (C−N), 1321 (NO_2 sym), 1561 (NO_2 asym), 1597 (C=C), 1717 (−C=O), 3307 (N−H).

Complex **2** *(**LH**$^+$·SO_4^{2-}·TBA$^+$·3H_2O).* Complex **2** was obtained as single crystals suitable for X-ray diffraction (XRD) analysis by adding an excess of $TBAHSO_4$ (10 equiv) to a 15 mL acetone suspension of receptor **L**. After the addition of $TBAHSO_4$, the suspension was stirred for about 1 h at room temperature, upon which a clear solution formed. The resulting solution was filtered into a test tube and allowed to slowly evaporate at room temperature, which yielded yellow crystals suitable for X-ray crystallography analysis within 20 days. Mp: 158 °C, ^{1}H NMR (d_6-DMSO): δ (ppm) 9.60 (s, 3H−N), 8.95 (s, 3H−N), 8.12 (d, 2H, J = 9.2 Hz, ArCH), 7.67 (d, 6H, J = 9.2 Hz, ArCH), 7.36 (d, 6H, J = 8.8 Hz, ArCH), 6.83 (d, 6H, J = 8.8 Hz, ArCH), 4.06 (s(br), 6H, NCH_2) 3.15 (m(br), 18H TBA−N$^+$$CH_2$ and NCH_2), 1.55 (s(br), 8H TBA−CH_2), 1.26 (q, J = 7.2 Hz, 8H, TBA−CH_2), 0.92 (t, 12H, J = 7.2 Hz, TBA−CH_3). FT-IR (ν, cm^{-1}): 1201 (C−N), 1335 (NO_2 sym), 1556 (NO_2 asym), 1601 (C=C), 1714 (−C=O).

Complex **3** *(**L**·2K$^+$·HPO_4^{2-}·23H_2O).* Complex **3** was obtained by adding a previously prepared 3 mL aqueous solution of K_2HPO_4 (36 mg 0.2 mmol) to an 8 mL DMSO solution of **L** (185 mg, 0.2 mmol). After the addition of aqueous K_2HPO_4, the mixture was stirred for about 1 h at room temperature. The resulting turbid mixture was filtered into a 20 mL conical flask and allowed to slowly evaporate for crystallization at room temperature, which yielded tiny pale yellow crystals suitable for X-ray crystallography analysis within 15 days. Mp: 198 °C. ^{1}H NMR (d_6-DMSO): δ (ppm) 9.69 (s, 3H−N), 9.02 (s, 3H−N), 8.11 (d, 6H, J = 9.2 Hz, ArCH), 7.66 (d, 6H, J = 9.2 Hz, ArCH), 7.36 (d, 6H, J = 8.8 Hz, ArCH), 6.83 (d, 6H, J = 8.4 Hz, ArCH), 4.01 (t, 6H, J = 5.6 Hz, NCH_2) 3.00 (t, 6H, J = 5.2 Hz, NCH_2),2H), FT-IR (ν, cm^{-1}): 1213 (C−N), 1333 (NO_2 sym), 1571 (NO_2 asym), 1604 (C=C), 1706 (−C=O), 3402 (N−H).

Complex **4** *(**L**·CO_3^{2-}·2TEA$^+$).* Complex **4** was obtained as single crystals suitable for X-ray diffraction (XRD) analysis by adding an excess of $TEAHCO_3$ (10 equiv) to a 5 mL DMSO solution of receptor **L**. After the addition of $TEAHCO_3$, the suspension was stirred for about 1 h at room temperature. The resulting red solution was filtered into a test tube and allowed to slowly evaporate at room temperature, which yielded red crystals suitable for X-ray crystallography analysis within 5 days. Mp: 168 °C. ^{1}H NMR (d_6-DMSO): δ (ppm) 8.09 (s (br), 6H, ArCH), 7.74 (s (br) 6H), 7.40 (s (br), 6H, ArCH), 6.72 (s (br), 6H, ArCH), 4.00 (s(br), 6H, NCH_2) 3.16 (s(br), 6H, NCH_2). FT-IR (ν, cm^{-1}): 1222 (C−N), 1313 (NO_2 sym), 1560 (NO_2 asym), 1604 (C=C), 1708 (−C=O), 3368 (N−H), 3454 (N−H).

Crystallographic Refinement Details. The crystallographic data and details of data collection for receptor **L** and its complexes **1**−**4** are given in Table 2. In each case, a crystal of suitable size was selected from the mother liquor, immersed in silicone oil, and then mounted on the tip of a glass fiber and cemented using resin. Intensity data for the crystals were collected with Mo Kα radiation (λ = 0.71073 Å) at 298(2) K, with increasing ω (width of 0.3° per frame) at a scan speed of 6 s/frame on a single-crystal X-ray diffractometer equipped with a CCD area detector. The data integration and reduction were processed with SAINT[12] software. An empirical absorption correction was applied to the collected reflections with SADABS.[13] The structures were solved by direct methods using SHELXTL[14] and were refined on F^2 by full-matrix least-squares techniques using the SHELXL-97 program package.[15] Graphics were generated using MERCURY 3.0

and ORTEP-3 for Windows.[16] In all cases, non-hydrogen atoms were treated anisotropically. Wherever possible, the hydrogen atoms were located on a difference Fourier map and refined. In other cases, the hydrogen atoms were geometrically fixed. Crystals of **L** and complex **2** included highly disordered and diffuse solvent molecules that could not be properly modeled. The corresponding residual electron density in these structures was treated with the SQUEEZE routine in PLATON,[17] which removed its contribution from the final *hkl* files. Similarly, for complex **4** the highly disordered two TEA countercations were treated as diffuse contributions to the overall scattering without specific atom positions by SQUEEZE/PLATON.[17] The presence of two TEA countercations was supported by the ^{1}H NMR spectrum recorded for crystals of complex **4**.

NMR Studies. ^{1}H NMR titration studies were done to determine the binding constants of **L** with different oxyanions in d_6-DMSO at room temperature. Initial concentrations were $[\text{ligand}]_0 = 5$ mM and $[\text{anion}]_0 = 50$ mM. Each titration was performed by 10−15 measurements at room temperature. The association constant log *K* was calculated by fitting urea NH signals using the EQNMR program.[11]

■ ASSOCIATED CONTENT

Ⓢ Supporting Information

Figures, a table, and CIF files giving characterization data for the receptor **L** and its complexes **1**−**4**, IR spectra, ^{13}C NMR and ^{1}H NMR spectra, ^{1}H NMR titration stack plots, fit plots, LC-MS, crystallographic data, distance vs angle plots, and hydrogen-bonding data. This material is available free of charge via the Internet at http://pubs.acs.org.

■ AUTHOR INFORMATION

Corresponding Author

*G.D.: tel, +91-361-2582313; fax, +91-361-2582349; e-mail, gdas@iitg.ernet.in.

Notes

The authors declare no competing financial interest.

■ ACKNOWLEDGMENTS

G.D. gratefully acknowledges the Council of Scientific and Industrial Research (01/2727/13/EMR-II) and Science & Engineering Research Board (SR/S1/OC-62/2011), New Delhi, India, for financial support. We thank the CIF, Department of Chemistry IIT Guwahati, and DST-FIST for research support. A.B. thanks IIT Guwahati for a fellowship.

■ REFERENCES

(1) (a) *Supramolecular Chemistry of Anions*; Bianchi, A., Bowman-James, K., García-España, E., Eds.; Wiley-VCH: Weinheim, Germany, 1997. (b) Beer, P. D.; Gale, P. A. *Angew. Chem.* **2001**, *113*, 502−532; *Angew. Chem., Int. Ed.* **2001**, *40*, 486−516. (c) Gale, P. A. *Coord. Chem. Rev.* **2003**, *240*, 191−221. (d) Gale, P. A. In *The Encyclopedia of Supramolecular Chemistry*; Atwood, J. L., Steed, J. W., Eds.; Marcel Dekker: New York, 2004; pp 31−41. (e) Smith, B. D. Ion-pair Recognition by Ditopic Receptors. *Macrocyclic Chemistry: Current Trends and Future perspectives*; Gloe, K., Antonioli, B., Eds.; Kluwer: London, 2005; pp 137−151. (f) *Anion Receptor Chemistry*; Sessler, J. L., Gale, P. A., Cho, W.-S., Eds.; RSC: Cambridge, U.K., 2006. (g) Gale, P. A.; Quesada, R. *Coord. Chem. Rev.* **2006**, *250*, 3219−3244. (h) Yoon, J.; Kim, S. K.; Singh, N. J.; Kim, K. S. *Chem. Soc. Rev.* **2006**, *35*, 355−360. (i) Gale, P. A.; García-Garrido, S. E.; Garric, J. *Chem. Soc. Rev.* **2008**, *37*, 151−190. (j) Caltagirone, C.; Gale, P. A. *Chem. Soc. Rev.* **2009**, *38*, 520−563. (k) Kim, S. K.; Sessler, J. L. *Chem. Soc. Rev.* **2010**, *39*, 3784−3809. (l) Gale, P. A. *Chem. Soc. Rev.* **2010**, *39*, 3746−3771. (m) Wenzel, M.; Hiscock, J. R.; Gale, P. A. *Chem. Soc. Rev.* **2012**, *41*, 480−520. (n) McConnell, A. J.; Beer, P. D. *Angew. Chem., Int. Ed.* **2012**, *51*, 5052−5061.

(2) (a) Ravikumar, I.; Ghosh, P. *Chem. Soc. Rev.* **2012**, *41*, 3077−3098. (b) Jia, C.; Wu, B.; Li, S.; Huang, X.; Zhao, Q.; Li, Q.-S.; Yang, X.-J. *Angew. Chem., Int. Ed.* **2011**, *50*, 486−490. (c) Custelcean, R.; Bock, A.; Moyer, B. A. *J. Am. Chem. Soc.* **2010**, *132*, 7177−7185. (d) Wu, B.; Liang, J.; Yang, J.; Jia, C.; Yang, X.- J.; Zhang, H.; Tang, N.; Janiak, C. *Chem. Commun.* **2008**, 1762−1764. (e) Lakshminarayanan, P. S.; Ravikumar, I.; Suresh, E.; Ghosh, P. *Chem. Commun.* **2007**, 5214−5216. (f) Dey, S. K.; Das, G. *Dalton Trans.* **2011**, *40*, 12048−12051. (g) Dey, S. K.; Das, G. *Dalton Trans.* **2012**, *41*, 8960−8972. (h) Akhuli, B.; Ravikumar, I.; Ghosh, P. *Chem. Sci.* **2012**, *3*, 1522−1530. (i) Dey, S. K.; Chutia, R.; Das, G. *Inorg. Chem.* **2012**, *51*, 1727−1738. (j) Gunnlaugsson, T.; Kruger, P. E.; Jensen, P.; Pfeffer, F. M.; Hussey, G. M. *Tetrahedron Lett.* **2003**, *44*, 8909−8913. (k) Brooks, S. J.; García-Garrido, S. E.; Light, M. E.; Cole, P. A.; Gale, P. A. *Chem. Eur. J.* **2007**, *13*, 3320−3329. (l) Brooks, S. J.; Gale, P. A.; Light, M. E. *Chem. Commun.* **2006**, 4344−4346. (m) Ravikumar, I.; Ghosh, P. *Chem. Commun.* **2010**, *46*, 1082−1084. (n) Pramanik, A.; Khansari, M. E.; Powell, D. R.; Fronczek, F. R.; Hossain, M. A. *Org. Lett.* **2014**, *16*, 366−369.

(3) (a) Rajbanshi, A.; Moyer, B. A.; Custelcean, R. *Cryst. Growth Des.* **2011**, *11*, 2702−2706. (b) Chutia, R.; Dey, S. K.; Das, G. *CrystEngComm* **2013**, *15*, 9641−9647.

(4) (a) Alajarin, M.; Orenes, R.-A.; Steed, J. W.; Pastor, A. *Chem. Commun.* **2010**, *46*, 1394−1403. (b) Koblenz, T. S.; Wassenaar, J.; Reek, J. N. H. *Chem. Soc. Rev.* **2008**, *37*, 247−262. (c) Yoshizawa, M.; Klosterman, J. K.; Fujita, M. *Angew. Chem., Int. Ed.* **2009**, *48*, 3418−3438. (d) Rebek, J., Jr. *Angew. Chem., Int. Ed.* **2005**, *44*, 2068−2078. (e) Lützen, A. *Angew. Chem., Int. Ed.* **2005**, *44*, 1000−1002. (f) González, J. J.; Ferdani, R.; Albertini, E.; Blasco, J. M.; Arduini, A.; Pochini, A.; Prados, P.; Mendoza, J. de. *Chem. Eur. J.* **2000**, *6*, 73−80. (g) Rudzevich, Y.; Rudzevich, V.; Schollmeyer, D.; Thondorf, I.; Böhmer, V. *Org. Lett.* **2005**, *7*, 613−616. (h) Deng, C.; Fang, R.; Guan, Y.; Jiang, J.; Lin, C.; Wang, L. *Chem. Commun.* **2012**, *48*, 7973−7975. (i) Singh, A. S.; Chen, B.-Y.; Wen, Y-S; Tsai, C.; Sun, S.-S. *Org. Lett.* **2009**, *11*, 1867−1870. (j) Singh, A. S.; Sun, S.-S. *Chem. Commun.* **2011**, *47*, 8563−8565.

(5) (a) Arunachalam, M.; Ghosh, P. *Chem. Commun.* **2011**, *47*, 8477−8492. (b) Custelcean, R. *Chem. Commun.* **2013**, *49*, 2173−2182. (c) Gale, P. A. *Acc. Chem. Res.* **2006**, *39*, 465−475. (d) Busschaert, N.; Wenzel, M.; Light, M. E.; Iglesias-Hernandez, P.; Perez-Tomas, R.; Gale, P. A. *J. Am. Chem. Soc.* **2011**, *133*, 14136−14148. (e) Basu, A.; Das, G. *Dalton Trans.* **2012**, *41*, 10792−10802. (f) Basu, A.; Das, G. *Chem. Commun.* **2013**, *49*, 3997−3999. (g) Arunachalam, M.; Ghosh, P. *Chem. Commun.* **2009**, 5389−5391.

(6) (a) Seidel, S. R.; Stang, P. J. *Acc. Chem. Res.* **2002**, *35*, 972−983. (b) Yang, Z.; Wu, B.; Huang, X.; Liu, Y.; Li, S.; Xia, Y.; Jia, C.; Yanga, X.-J. *Chem. Commun.* **2011**, *47*, 2880−2882. (c) Akhuli, B.; Ghosh, P. *Dalton Trans.* **2013**, *42*, 5818−5825. (d) Turner, D.; Hursthouse, R. M. B.; Light, M. E.; Steed, J. W. *Chem. Commun.* **2004**, 1354−1355. (e) Custelcean, R.; Bonnesen, P. V.; Roach, B. D.; Duncan, N. C. *Chem. Commun.* **2012**, *48*, 7438−7440. (f) Li, S.; Jia, C.; Wu, B.; Luo, Q.; Huang, X.; Yang, Z.; Li, Q.-S.; Yang, X.-J. *Angew. Chem., Int. Ed.* **2011**, *50*, 5721−5724. (g) Custelcean, R.; Bonnesen, P. V.; Duncan, N. C.; Zhang, X.; Watson, L. A.; Berkel, G. V.; Parson, W. B.; Hay, B. P. *J. Am. Chem. Soc.* **2012**, *134*, 8525−8534.

(7) Dey, S. K.; Das, G. *Cryst. Growth Des.* **2009**, *10*, 750−760.

(8) Dutta, B. K.; Kar, C.; Basu, A.; Das, G. *Tetrahedron Lett.* **2013**, *54*, 771−774.

(9) Hay, B. P.; Firman, T. K.; Moyer, B. A. *J. Am. Chem. Soc.* **2005**, *127*, 1810−1819.

(10) (a) Wang, T.; Yan, X.-P. *Chem. Eur. J.* **2010**, *16*, 4639−4649. (b) Maeda, H.; Kusunose, Y. *Chem. Eur. J.* **2005**, *11*, 5661−5666. (c) Brooks, S. J.; Gale, P. A.; Light, M. E. *CrystEngComm* **2005**, *7*, 586−591. (d) Juwarker, H.; Jeong, K.-S. *Chem. Soc. Rev.* **2010**, *39*, 3664−3674. (e) Basu, A.; Das, G. *Inorg. Chem.* **2012**, *51*, 882−889.

(11) Hynes, M. J. *J. Chem. Soc., Dalton Trans.* **1993**, 311−312.

(12) Sheldrick, G. M. *SAINT and XPREP, 5.1 ed.*; Siemens Industrial Automation Inc., Madison, WI, 1995.

(13) Sheldrick, G. M. *SADABS, Empirical Absorption Correction Program*; University of Göttingen, Göttingen, Germany, 1997.

(14) Sheldrick, G. M. *SHELXTL Reference Manual: Version 5.1*; Bruker AXS: Madison, WI, 1997.

(15) Sheldrick, G. M. *SHELXL-97: Program for Crystal Structure Refinement*; University of Göttingen, Göttingen, Germany, 1997.

(16) (a) *Mercury 3.0* (supplied with Cambridge Structural Database); CCDC, Cambridge, U.K., 2011−2012. (b) Farrugia, L. J. *J. Appl. Crystallogr.* **1997**, *30*, 565.

(17) Sluis, P. V. D.; Spek, A. L. *Acta Crystallogr.* **1990**, *A46*, 194.